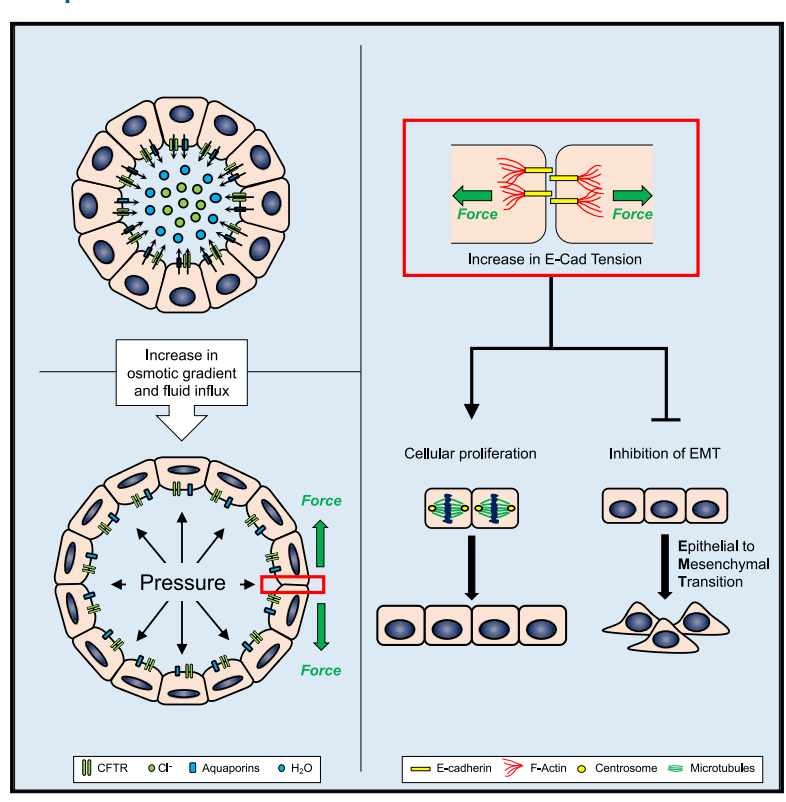
Current Biology

Osmotic Gradients in Epithelial Acini Increase Mechanical Tension across E-cadherin, Drive Morphogenesis, and Maintain Homeostasis

Graphical Abstract



Authors

Vani Narayanan, Laurel E. Schappell, Carl R. Mayer, ..., Kris N. Dahl, Jason P. Gleghorn, Daniel E. Conway

Correspondence

dconway@vcu.edu

In Brief

Narayanan et al. describe the role of ion secretion in the generation of osmotic pressure and changes in mechanical tension across E-cadherin in epithelial acini. Increasing the osmotic gradient increased force exerted across E-cadherin, induced cellular proliferation, and blocked EMT progression.

Highlights

- E-cadherin experiences higher mechanical tension in acini compared with monolayers
- E-cadherin tension is positively correlated to CFTR activity
- Epithelial acini have significant lumen pressure due, in part, to CFTR activity
- Increased CFTR activity increases cell proliferation and blocks EMT progression







Osmotic Gradients in Epithelial Acini Increase Mechanical Tension across E-cadherin, Drive Morphogenesis, and Maintain Homeostasis

Vani Narayanan,¹ Laurel E. Schappell,² Carl R. Mayer,¹ Ashley A. Duke,¹ Travis J. Armiger,³ Paul T. Arsenovic,¹ Abhinav Mohan,¹ Kris N. Dahl,³ Jason P. Gleghorn,² and Daniel E. Conway^{1,4,*}

¹Department of Biomedical Engineering, Virginia Commonwealth University, Richmond, VA 23284, USA

*Correspondence: dconway@vcu.edu https://doi.org/10.1016/j.cub.2019.12.025

SUMMARY

Epithelial cells spontaneously form acini (also known as cysts or spheroids) with a single, fluidfilled central lumen when grown in 3D matrices. The size of the lumen is dependent on apical secretion of chloride ions, most notably by the CFTR channel, which has been suggested to establish pressure in the lumen due to water influx. To study the cellular biomechanics of acini morphogenesis and homeostasis, MDCK-2 cells. Using FRET-force biosensors for E-cadherin, we observed significant increases in the average tension per molecule for each protein in mature 3D acini as compared to 2D monolayers. Increases in CFTR activity resulted in increased E-cadherin forces, indicating that ionic gradients affect cellular tension. Direct measurements of pressure revealed that mature acini experience significant internal hydrostatic pressure (37 ± 10.9 Pa). Changes in CFTR activity resulted in pressure and/or volume changes, both of which affect E-cadherin tension. Increases in CFTR chloride secretion also induced YAP signaling and cellular proliferation. In order to recapitulate disruption of acinar homeostasis, we induced epithelial-tomesenchymal transition (EMT). During the initial stages of EMT, there was a gradual decrease in E-cadherin force and lumen pressure that correlated with lumen infilling. Strikingly, increasing CFTR activity was sufficient to block EMT. Our results show that ion secretion is an important regulator of morphogenesis and homeostasis in epithelial acini. Furthermore, this work demonstrates that, for closed 3D cellular systems, ion gradients can generate osmotic pressure or volume changes, both of which result in increased cellular tension.

INTRODUCTION

While some epithelial tissues exist as continuous sheets of cells, in many organs, they form more elaborate three-dimensional (3D) structures, such as tubes or ducts with single lumens that transport gases and liquids. Epithelial cells cultured in reconstituted basement membranes or collagen gels spontaneously form acini (also known as cysts or spheroids) with a single hollow lumen that resembles 3D epithelial structures found in normal tissue [1]. Acinar cells exhibit differences in both apical-basal polarity and responses to growth factors when compared to cells grown as 2D monolayers [1]. Differences in cell-cell junctions, cytoskeletal organization, and nuclear shape [2] have also been reported, suggesting that cellular response to mechanical cues could be different in 3D acini.

Ionic gradients established across cellular membranes facilitate fluid secretion into epithelial lumens. The resulting hydrostatic pressure that arises from fluid influx has been identified as a key regulator of embryogenesis and organ development [3, 4]. Prior studies have established that a chloride channel known as cystic fibrosis transmembrane conductance regulator (CFTR) regulates the lumen size of epithelial acini [5, 6]. CFTR contains numerous protein kinase A (PKA) and protein kinase C (PKC) phosphorylation sites that regulate the activity of the channel [7]. Based on the relationship between CFTR activity and lumen size, it has been hypothesized that changes in apical delivery of ions by pumps and channels would create an osmotic pressure within the lumen of acini [8]. Recent computational models of lumenogenesis have shown that hydrostatic pressure (formed by the equilibrium of osmotic pressure, fluid influx, and paracellular leak) contribute to lumen growth and homeostasis

An essential aspect of 3D epithelial morphogenesis and homeostasis is attributed to the formation and maintenance of cell-cell junctions [11, 12]. E-cadherin has been shown to mediate lumen formation in acinar structures [13, 14]. Modulation of E-cadherin adhesion [15], and overexpression of cadherin-6 have shown to impair tubulogenesis [13]. Significant rearrangements in adherens junctions, desmosomes, and tight junctions have been observed during tubulogenesis [16]. Lastly, changes in expression of cell-cell adhesion molecules have been



²Department of Biomedical Engineering, University of Delaware, Newark, DE 19716, USA

³Department of Chemical Engineering, Carnegie Mellon University, Pittsburgh, PA 15213, USA

⁴Lead Contact

established as one of the hallmarks of epithelial-to-mesenchymal transition (EMT) progression. Taken together, these observations point to cell-cell contacts as an important mediator of acini homeostasis and morphogenesis.

Recent work by our group and others has shown that E-cadherin is subjected to significant mechanical force in 2D monolayers [17, 18]. Given the significant differences in epithelial cell behavior between 2D and 3D, as well as the important role of cell-cell contacts in 3D epithelial morphogenesis and homeostasis, we hypothesized that the mechanical forces at adherens junctions in 3D acini would be substantially different from the forces in 2D monolayers. In this study, we used two approaches to study the biomechanics of acini, using Madin-Darby canine kidney (MDCK) epithelial cells as a model system. First, using previously developed and validated fluorescence resonance energy transfer (FRET)-force biosensors, we observed a significant increase in tension across E-cadherin in 3D acini compared to 2D monolayers. E-cadherin tension was proportional to CFTR activity, indicating that ionic gradients increase mechanical forces between cells. Second, using a micropipette device, we directly measured the internal pressure in the lumen of acini. Mature acini had substantial pressure (37 Pa), which was dependent on CFTR activity. We also show that changes in osmotic gradients are correlated to lumen formation, cell proliferation, and EMT progression. Taken together, our data show that ionic gradients induce cellular forces that regulate the morphogenesis and homeostasis of epithelial acini.

RESULTS

Significant Mechanical Forces Are Present in Mature Epithelial Acini

To study the cellular biomechanics of epithelial acini, we developed a MDCK-2 cell line stably expressing previously developed E-cadherin [18]. The FRET biosensors use the TSmod sensor (Figures S1A and S1B), which has an inverse FRET-force relationship [19]. Initial experiments were performed with cells growing in or on top of Matrigel in order to form acini and 2D monolayers, respectively, over a period of 7 to 10 days. The acinar structures consisted of a sphere with a single hollow lumen with distribution of the E-cadherin force sensor similar to that of endogenous E-cadherin (Figures S1C and S1D), which is consistent with previous publications [20, 21]. Acini expressing the E-cadherin tension sensor displayed reduced FRET compared to 2D monolayers grown on Matrigel, indicating an increase in force across E-cadherin in 3D structures (Figure 1A). While we felt it best to compare the biophysical behavior in 2D versus 3D using the same matrix, we note that Matrigel is a soft matrix (estimated to be 450 Pa) [22]. We have previously shown that cells grown on 1-kPa gels have reduced E-cadherin tension [17]; therefore, 2D monolayer data in Figure 1A should not be compared to prior 2D work with cells cultured on plastic or glass [17, 18, 23]. Additionally, FRET measurements made using a force-insensitive control for E-cadherin (Ecad∆cyto) did not show significant differences in forces exerted across E-cadherin in 3D compared to 2D structures (Figure 1B; Figures S1A and S1B).

To further confirm that reduced FRET in 3D conditions was due to increased force, we performed a number of control experiments. First, we examined whether the cell junction orientation

in 3D conditions (flipped 90° from 2D) contributed to the FRET differences. We imaged both the equatorial and bottom regions of individual acini, noting that the bottom regions of the acinus were more similar to the junction orientation in 2D conditions. There were no significant differences between equatorial and bottom junctions in 3D acini (Figure 1C). Second, we considered the possibility that changes in cadherin clustering could affect intermolecular FRET (non-force FRET occurring between adjacent sensors). We developed a stable cell line expressing both an E-cadherin tension sensor with a "dark" donor (mTFP1) and also an E-cadherin tension sensor with a "dark" acceptor (mEYFP) to measure intermolecular FRET, similar to [24]. Intermolecular FRET was only a minimal component of FRET, and importantly, it did not change between 2D and 3D conditions (Figure S1E).

We speculated that tension across E-cadherin would change during the development of the acinus. We observed an increase in E-cadherin tension from immature acini (day 3) to mature acini (day 7) (Figure 1D). The increased forces correlated with the transition from a multiple lumen phenotype to the formation of a single lumen.

CFTR Activity Regulates Mechanical Tension across E-cadherin

To further test the hypothesis that ionic gradients affect E-cadherin tension, we examined how alterations in CFTR activity affected E-cadherin tension. To activate CFTR, cells were treated with forskolin (Fsk) to elevate cAMP (cyclic adenosine monophosphate) levels. Elevated cAMP levels activate PKA, ultimately leading to the activation of CFTR [25]. Fsk treatment for 24 h resulted in a significant increase in mechanical tension across E-cadherin (Figure 2A). In parallel experiments, we also used CFTR_{inh}-172 as a direct inhibitor of CFTR activity [26]. Treatment with CFTR_{inh}-172 reduced force across E-cadherin (Figure 2A). When cells were pre-treated with CFTR_{inh}-172 prior to the addition of Fsk, the force across E-cadherin was not affected by Fsk (Figure 2A), confirming that the effect of Fsk on E-cadherin force requires CFTR activity. Treatment of cells with CFTR_{inh}-172 after Fsk treatment did not completely reverse the Fsk-induced increase in E-cadherin force (Figure S2A), suggesting that established ionic gradients can persist in the absence of CFTR activity. Furthermore, FRET measurements made while using the force-insensitive control for E-cadherin (Ecad∆cyto) did not show any significant differences in force across E-cadherin in response to the activation and/or inhibition of CFTR activity (Figure 2B).

To genetically increase CFTR activity, we knocked down CSE1L, a known inhibitor of CFTR [27] (Figure S2D). After only 5 days, MDCK-2 cells expressing the E-cadherin tension sensor module with reduced CSE1L had a larger lumen and higher E-cadherin force compared to its non-silenced scramble control (Figure 2C), in agreement with prior results [27]. Additionally, treatment with CFTR_{inh}-172 rescued the effects of CSE1L knockdown, restoring E-cadherin forces to normal levels (Figure 2C). Acini with reduced CSE1L levels also had a multilayered structure, likely attributed to other functions of CSE1L, such as apoptosis [28] or cell polarity [29].

As an alternate approach to modulate the ionic gradient present in the lumen, we used the inhibitor ouabain to inhibit the

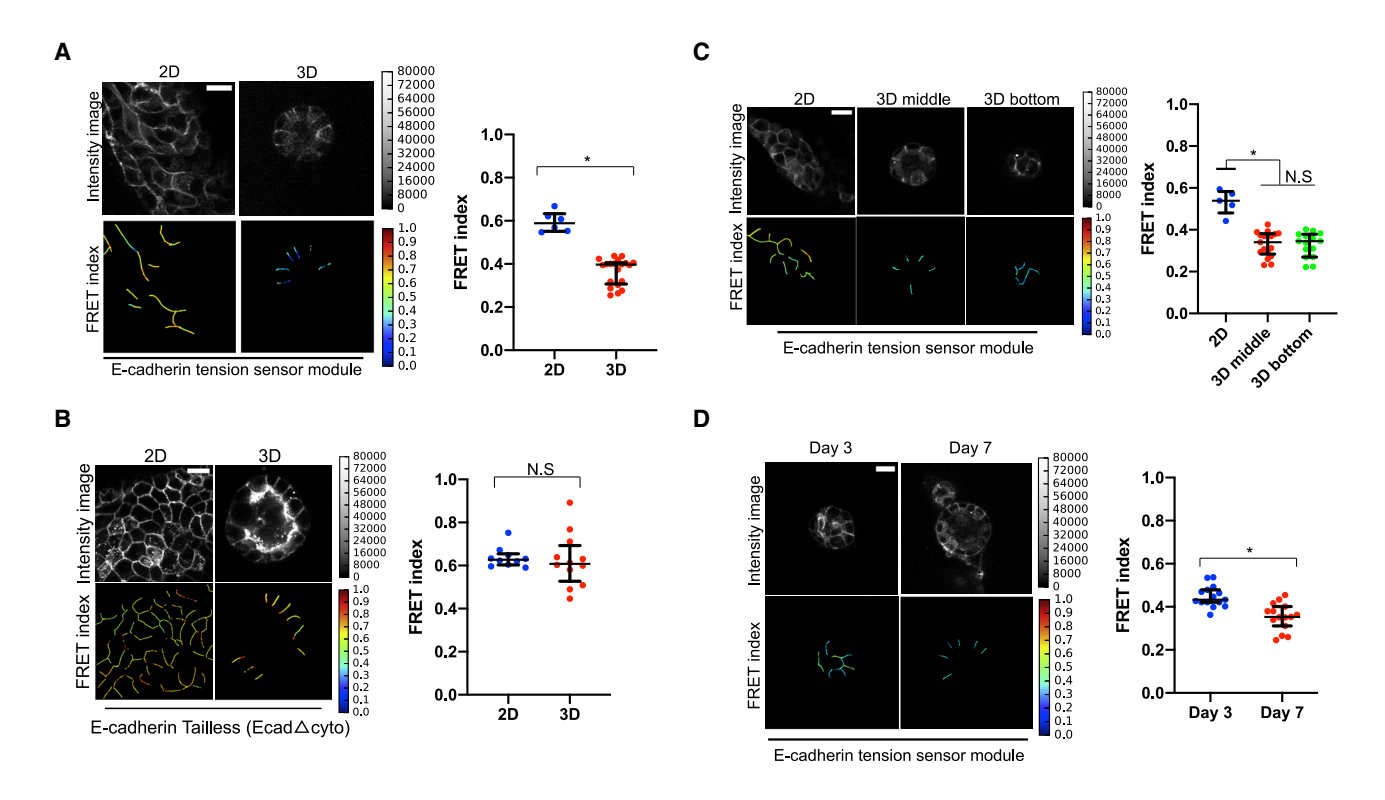


Figure 1. Epithelial Acini Experience Significant Osmotic Stretch in 3D

MDCK-2 cells expressing the E-cadherin tension sensor modules were used in all experiments.

(A) Cells expressing the full-length E-cadherin tension sensor module were grown in Matrigel to form 3D acini or on top of Matrigel to form a 2D monolayer (scale bar, 20 μ m). The scatter dot plot shows FRET index measurements across multiple acini depicting a significantly higher force across E-cadherin in 3D acini as compared to monolayers. The horizontal line (black) in the scatter dot plot denotes the median of the FRET index estimates, and the whiskers denote the largest observation within 1.5 × interquartile range (IQR) (representative data shown is from one experiment out of a total of three independent experiments performed on separate days; *p < 0.05, Mann-Whitney test).

(B) FRET index measurements in the force-insensitive tailless control (EcadΔcyto) shows no difference in force across E-cadherin in acini compared to monolayers (scale bar, 20 μm). The horizontal line (black) denotes the median of the FRET index estimates, and the whiskers denote the largest observation within 1.5 × IQR (representative data shown are from one experiment out of a total of three independent experiments performed on separate days; N.S, not significant, p > 0.05, Mann-Whitney test).

(C) FRET index measurements to analyze E-cadherin FRET based on cell-cell junction orientation in acini. Data shown as FRET index images and scatter dot plot depicts no significant difference in FRET across cell-cell junctions in a bottom slice of the acinus compared to the middle section (scale bar, 20 μ m). The horizontal line (black) denotes the median of the FRET index estimates, and the whiskers denote the largest observation within 1.5 × IQR (representative data shown are from one experiment out of a total of three independent experiments performed on separate days; *p < 0.05, one-way ANOVA test and Mann-Whitney test; N.S, not significant, p > 0.05).

(D) Multiple acini expressing the full-length E-cadherin tension sensor showed a significant decrease in FRET on day 7 of acini morphogenesis (indicating higher E-cadherin force), wherein acini exhibited single-lumen morphology as compared to day 3 on which a multiple lumen phenotype was depicted (scale bar, 20 µm). The scatter dot plot of the FRET index measurements depicts a higher force (lower FRET) on day 7 as compared to day 3 of acini morphogenesis. The horizontal line (black) denotes the median of the FRET index estimates, and the whiskers denote the largest observation within 1.5 × IQR (representative data shown is from one experiment out of a total of three independent experiments performed on separate days; *p < 0.05, Mann-Whitney test). See also Figure S1 for validation of the tension sensor modules used in the experiments.

basal Na⁺/K⁺-ATPase pump, which is essential for regulating solute and fluid transport into the cell and acinar lumen size [30, 31]. Inhibition of the Na⁺/K⁺-ATPase via ouabain reduced force across E-cadherin compared to the untreated control (Figure 2D).

We also observed variation in the localization of E-cadherin with a number of pharmacological treatments (Figures 2A and 2D). Masking of cells was carefully performed to remove intracellular E-cadherin from FRET analysis. Minimal intermolecular FRET was observed in all treatments with no significant differences between groups (Figure S2B). Additionally, we also examined the effects of Fsk, PKA agonist (8-bromo cAMP), and

CFTR_{inh}-172 in 2D monolayer cultures, which also similarly affected E-cadherin localization and expression. These treatments did not affect FRET in 2D monolayers (Figure S2C), suggesting that a closed 3D system is necessary for these conditions to affect force exerted across E-cadherin.

CFTR Activity Affects Acini Pressure and Deformability

To directly measure hydrostatic pressure within the acinar lumen, we used a custom micropipette system in which the relative internal lumen pressure of a single acinus was measured (see example trace in Figure S3A). In mature acini, we measured pressure of 37 \pm 10.9 Pa (Figure 3A). Inhibition of

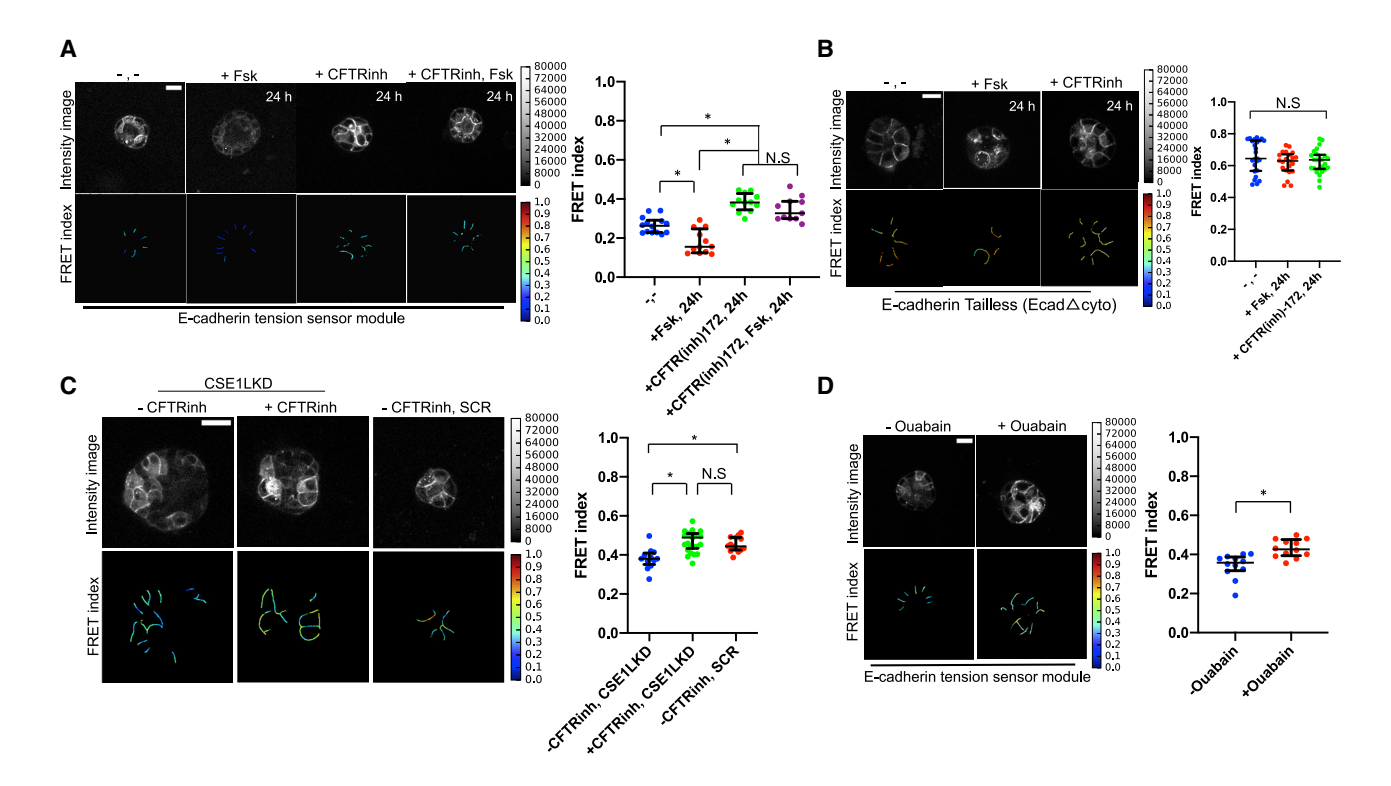


Figure 2. Osmotic Pressure Drives Force across E-cadherin in Epithelial Acini

MDCK-2 cells expressing the E-cadherin tension sensor modules were used in all experiments.

(A) Acini expressing the E-cadherin tension sensor module were treated with Fsk (10 μ M) for 24 h and showed significant decrease in FRET indicating higher force. CFTR_{inh}-172 treatment (10 μ M) significantly reduced force across E-cadherin. The scatter dot plot shows FRET index measurements across multiple acini depicting a significantly higher force across E-cadherin upon Fsk treatment over a period of 24 h as compared to the untreated control and acini that were CFTR inhibited. Fsk treatment following CFTR inhibition seldom caused any change in the reduced force. The horizontal line (black) denotes the median of the FRET index estimates, and the whiskers denote the largest observation within 1.5 × IQR (representative data shown are from one experiment chosen from a pool of three independent experiments performed on separate days; *p < 0.05; N.S, not significant, p > 0.05, one-way ANOVA and Mann-Whitney test). Scale bar, 20 μ m.

(B) Treatment of the truncated E-cadherin mutant (EcadΔcyto) with Fsk and CFTR(inh)-172 for 24 h did not yield any significant changes to FRET when compared to the untreated control (-,-), as shown in the FRET index images and scatter dot plot. The horizontal line (black) denotes the median of the FRET index estimates, and the black whiskers denote the largest observation within 1.5 × IQR (representative data shown are from one experiment chosen from a pool of three independent experiments that were performed on separate days; N.S, not significant, p > 0.05, one-way ANOVA and Mann-Whitney test). Scale bar, 20 μm.

(C) Significant increase in mechanical tension across E-cadherin (decreased FRET) and larger lumen size were detected in CSE1LKD (-CFTRinh, CSE1LKD) compared to control cells that were infected with a non-targeting short hairpin RNA (shRNA) (-CFTRinh, SCR) as well as the CFTR-inhibited CSE1LKD control (+CFTRinh, CSE1LKD), as shown in the scatter dot plot. The CFTR-inhibited control (+CFTRinh, CSE1LKD) was treated with the CFTR inhibitor (CFTR(inh)-172) on day 0, with media replenishment containing CFTR(inh)-172 every day until the fifth day of acinar development. The horizontal line (black) denotes the median of the FRET index estimates, and the black whiskers denote the largest observation within 1.5 × IQR (representative data shown are from one experiment chosen from a pool of three independent experiments that were performed on separate days; *p < 0.05; N.S, not significant, p > 0.05, one-way ANOVA and Mann-Whitney test). Scale bar, 50 μm.

(D) Effect of Na $^+$ / K $^+$ -ATPase inhibition on force across E-cadherin in epithelial acini. Acini treated with ouabain (Na $^+$ / K $^+$ -ATPase inhibitor, 0.1 μ M) showed significant increase in FRET (reduced force across E-cadherin) 48 h post-treatment compared to the untreated control. The ouabain-treated acini exhibited epithelial stratification, thereby showing a reduction in lumen size. The horizontal line (black) in the scatter dot plot denotes the median of the FRET index estimates, and the black whiskers denote the largest observation within 1.5 \times IQR (representative data shown are from one experiment chosen from a pool of three independent experiments that were performed on separate days; $^*p < 0.05$, Mann-Whitney test). Scale bar, 20 μ m.

See also Figure S2, which shows how perturbation of CFTR activity can modulate tension across E-cadherin in glandular acini.

CFTR (CFTR_{inh}-172) or the basal Na⁺/K⁺-ATPase (ouabain) for 24 h reduced pressure approximately 50% (Figure 3A; Figure S3B), indicating that ionic gradients significantly contribute to lumen pressure. Surprisingly, the activation of CFTR via Fsk or PKA agonist (8-bromo cAMP) for 24 h did not result in a significant increase in pressure (Figure 3A; Figure S3B). However, treatment with Fsk resulted in a significant increase in lumen diameter (Figures 3B and 3C). This suggests that further

increases in ionic gradients act to increase lumen size rather than lumen pressure.

To further investigate whether ionic gradients had a significant mechanical effect on the acinar structure, we compared the responses of control (–Fsk, –CFTR(inh)172), Fsk-treated (+Fsk, 24 h), and CFTR_{inh}-172-treated (+CFTR(inh)172, 24 h) acini to compression (Figure 3D; Figures S3C–S3H). We measured both the deformation under compression and elastic recoil

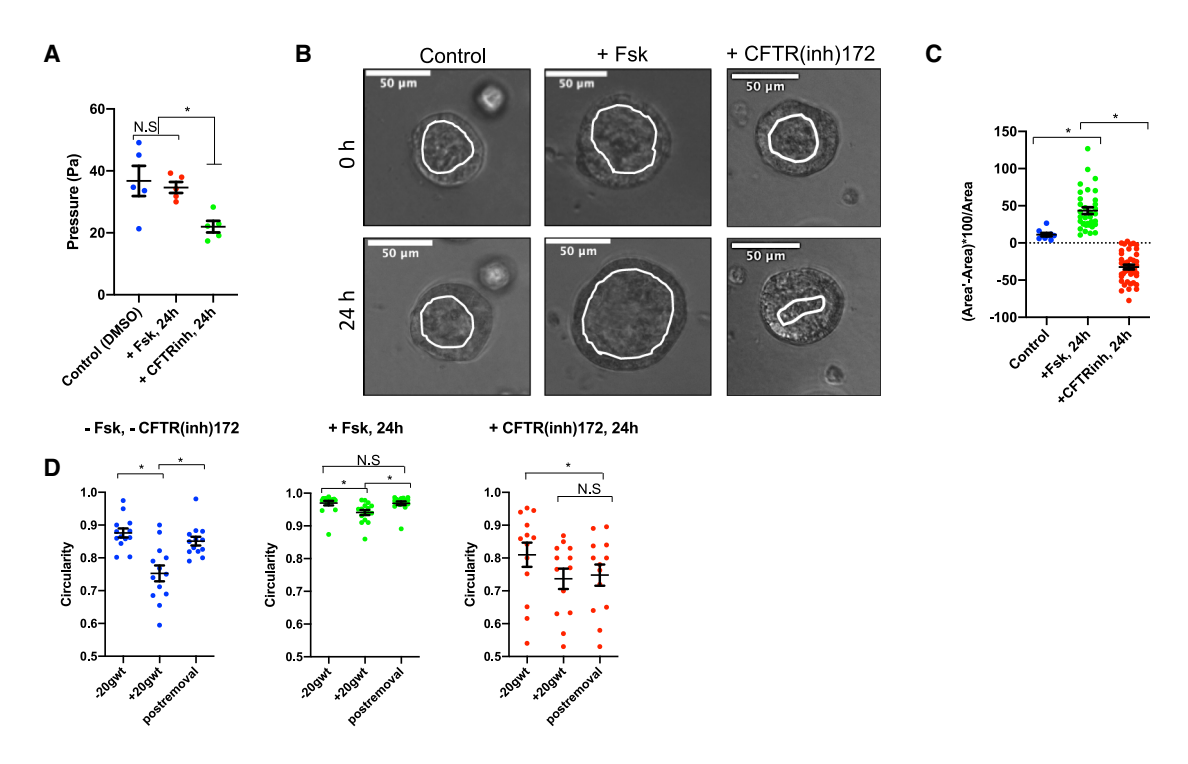


Figure 3. CFTR Activity Affects Lumen Pressure and Deformability in Epithelial Acini

(A) Lumen pressure was directly measured in acini. Acini were cultured in Matrigel until they reached a luminal diameter of approximately 200 μ m, and then pressure was measured following culture for 24 h in media containing Fsk (10 μ M), CFTR inhibitor (CFTR(inh)-172, 10 μ M), and vehicle control (DMSO). At least 5 acini were measured for pressure in all three cases (*p < 0.001; N.S., not significant, p > 0.05, one-way ANOVA, Tukey honestly significant difference [HSD] test). (B) MDCK-2 acini grown in Matrigel, on 8-well chamber slides for 6 days, were imaged prior to treatment, and the same acinus was located post the 24-h Fsk (10 μ M) and 24-h CFTR(inh)-172 (10 μ M) treatment for lumen area changes. Representative image shows the central cross-section of acini with the lumen circumference outlined (white). Scale bars, 50 μ m.

(C) Percent change in luminal area depicts a significant increase in luminal size after 24 h of Fsk treatment and a significant reduction in size after 24 h of CFTR(inh)-172 treatment, compared to the untreated control. At least 15 acini were scored for each group over two independent experiments (*p < 0.001, paired t test). (D) Significant reduction in circularity upon compression of acini expressing the E-cadherin tension sensor module with a 20-g calibrated weight, and higher elastic recoil to the original shape was observed in the untreated group ([-] CFTR_{inh}-172) compared to the Fsk-treated (+Fsk; 24 h) and the CFTR-inhibited (+CFTR(inh)-172; 24 h) groups. -20gwt indicates prior to compression, +20gwt denotes compression with weight, and postremoval denotes recovery after removal of weight. Data represent paired analysis (13 acini were scored for each group for all three cases; *p < 0.001, paired t test). Refer to Figure S3 to see how lumen pressure and acinar plasticity are affected through modulation of CFTR activity.

when the weight was removed to qualitatively assess the role of internal pressure in mediating the spherical shape. We observed larger deformations for control acini during compression (measured as changes in circularity and mean edge strain, respectively) (Figure 3D; Figures S3D, S3G. and S3H) as compared to acini treated with Fsk and CFTR_{inh}-172 (Figures S3E, S3F,and S3H). Additionally, we observed reduced recoil (measured as circularity) for CFTR-inhibited acini as compared to control and Fsk-treated acini (Figure 3D; Figure S3H). The lack of recoil in the CFTR-inhibited acini, the reduced deformation in Fsk-treated acini, and the increased circularity in uncompressed Fsk-treated acini indicate that lumen pressure is important for maintaining acinar shape and elasticity and for resisting deformation by external forces.

Osmotic Stretch Regulates E-cadherin-Force-Induced Proliferation

Based on prior studies, we hypothesized that the increased tension across E-cadherin, as a result of ionic gradients, induces proliferation in an E-cadherin-dependent manner [32]. To assess cellular proliferation, acini were stained with Ki-67. Fsk induced

nuclear localization of Ki-67 between 24 and 48 h in the non-transfected parental MDCK-2 acini. Ki-67 expression, however, was minimized in cells expressing a cytoskeletal decoupled "tailless" E-cadherin (EcadΔcyto) (Figure 4A; Figures S1A and S1B), indicating that cytoskeleton-connected E-cadherin is necessary for the response. Acini treated with Fsk for a period of 6 h showed a significant increase in positive YAP1 nuclear staining as early as 6 h compared to the control (Figures 4C and 4D). Fsk also did not increase Ki-67 as well as YAP1 expression in 2D monolayers (Figures S4A–S4D), indicating that the Fsk-mediated effects require a 3D environment to induce proliferation. Lastly, knockdown of CSE1L to increase CFTR activity also increased Ki-67 and YAP1 expression compared to the non-silenced control (Figures 4B, 4E, and 4F).

Mechanical Force across E-cadherin Is Downregulated during EMT Progression

Because EMT is known to affect acinar lumen morphology by inducing lumen filling, we wanted to understand how force exerted on E-cadherin is affected during the early stages of EMT, prior to downregulation of E-cadherin. First, we observed that

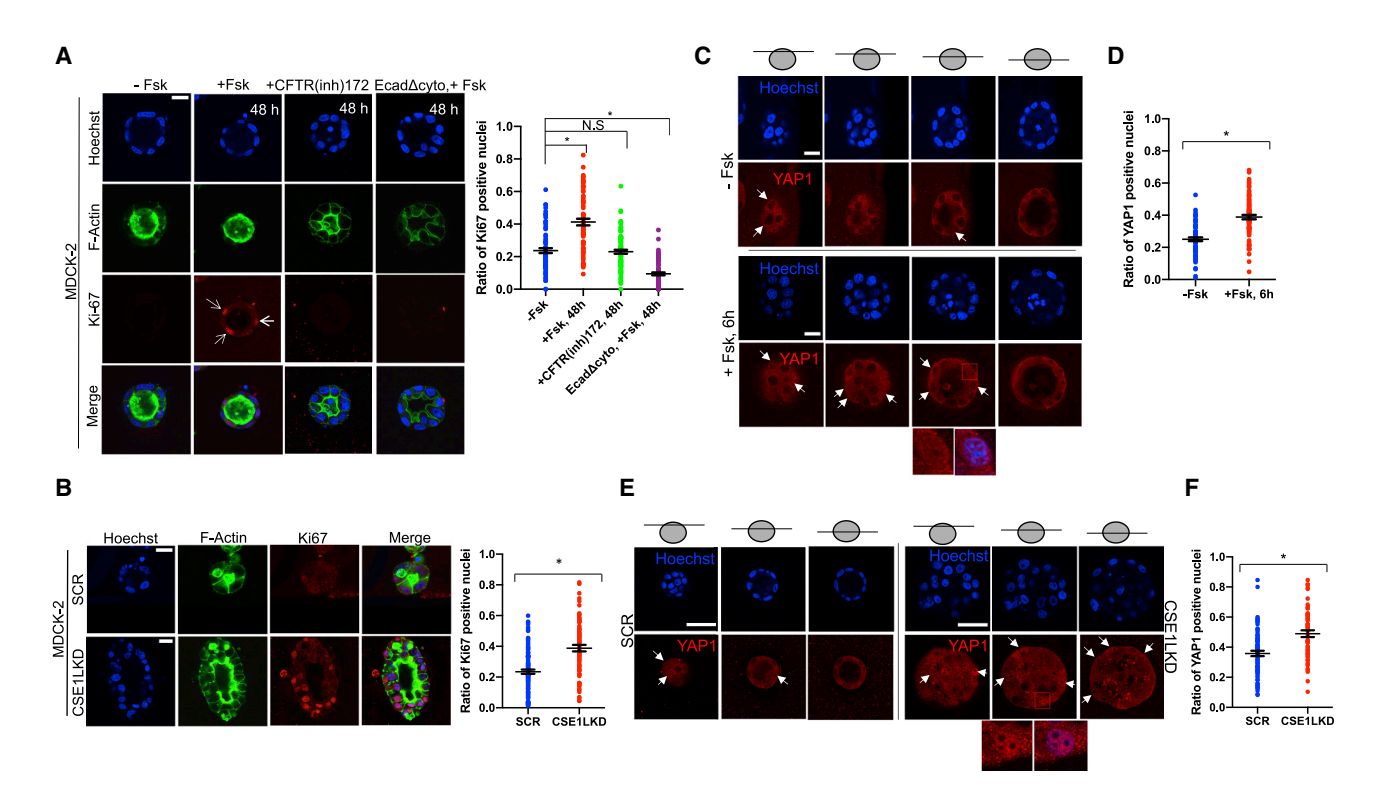


Figure 4. Osmotic Pressure Regulates Cellular Proliferation in an E-cadherin-Dependent Manner

MDCK-2 cells were used in all experiments.

(A) MDCK-2 parental cells were Ki-67 (red) positive after 48 h of treatment with Fsk. Fsk treatment of Ecad Δ cyto-expressing cells and CFTR inhibition did not induce cellular proliferation. Actin-488 was used to stain the actin cytoskeleton (green), and the nuclei were counterstained with Hoechst 33342 (blue). Quantification of immuno-positive nuclei (Ki-67) normalized against the total nuclei count is as shown. Representative data show the central cross-section of acini with and without treatment. At least 30 acini were scored over three independent experiments. Mean \pm SEM is indicated. *p < 0.001, one-way ANOVA, Tukey (HSD) test. Scale bar, 20 μ m.

(B) Cells with CSE1L knockdown had increased Ki-67 (red) staining as compared to scramble control (SCR) cells. All acini were fixed on day 5 and co-stained for actin (green), and the nuclei (blue) were counterstained with Hoechst 33342 (scale bars, 20 μm). Quantitative analysis of the number of proliferating cells as indicated by positive Ki-67 nuclear staining depicts a higher proportion of proliferating cells in the CSE1LKD compared to its non-silenced scramble control. Representative data show the central cross-section of acini with and without treatment. At least 30 acini were scored over three independent experiments. Mean ± SEM is indicated. *p < 0.001, Student's t test.

(C) MDCK-2 parental cells showed an increase in nuclear YAP localization (red) as early as 6 h post-treatment with forskolin. Representative data show four cross-sections of the acinus (from top to center) indicating active-YAP localization. The nuclei (blue) were counterstained with Hoechst 33342. Scale bars, 20 μm. (D) Quantification of immuno-positive nuclei (YAP1) normalized against the total nuclei count depicts a higher proportion of stretch-induced cells in the Fsk-treated group (+Fsk; 6 h) as compared to the untreated control (-Fsk). About 40 acini were scored over three independent experiments. Mean ± SEM is indicated. *p < 0.001, one-way ANOVA, Tukey (HSD) test.

(E) Cells with CSE1L knockdown (CSE1LKD) had increased YAP1 (red) staining as compared to scramble control (SCR) cells. Representative data show three cross-sections of the acinus (from top to center) indicating active-YAP localization. All acini were fixed on day 5, and the nuclei (blue) were counterstained with Hoechst 33342 (scale bars, 50 μm).

(F) Quantitative analysis of the number of YAP-positive nuclei as indicated by positive YAP nuclear staining depicts a higher proportion of stretch-induced cells in the CSE1LKD as compared to its non-silenced scramble control (SCR). At least 30 acini were scored over three independent experiments. Mean ± SEM is indicated. *p < 0.001, Student's t test.

Refer to Figure S4 to see how osmotic pressure-driven stretch is absent in epithelial monolayers.

mechanical force across E-cadherin, measured via FRET ratio analysis (Figures 5A and 5B) was gradually reduced over the course of 48 h of transforming growth factor $\beta 1$ (TGF- $\beta 1$)-induced EMT. We also observed a decrease in tensile force exerted across E-cadherin during EMT progression in 2D monolayers (Figure S5A). Measurement of lumen pressure showed an approximately 50% decrease in acini after 24 h of TGF- $\beta 1$ treatment (Figure 5C). To test the hypothesis that higher forces exerted on E-cadherin might prevent progression through EMT, we pre-treated the cells with Fsk prior to TGF- $\beta 1$

treatment. Fsk prevented TGF- β 1-induced changes in lumen morphology; force across E-cadherin; and expression of N-cadherin, α -smooth muscle actin, vimentin, and E-cadherin (Figures 5D–5F; and Figures S5B and S5C). Additionally, Fsk treatment also minimized Twist nuclear localization (Figure S5D), suggesting that TGF- β signaling is also regulated by changes in osmotic gradients. Because cAMP signaling has been shown to affect EMT [33], we compared the effects of PKA and Epac1 agonists on monolayers and acini to decouple the effects of osmotically driven stretch (present in acinar structures) from signaling effects

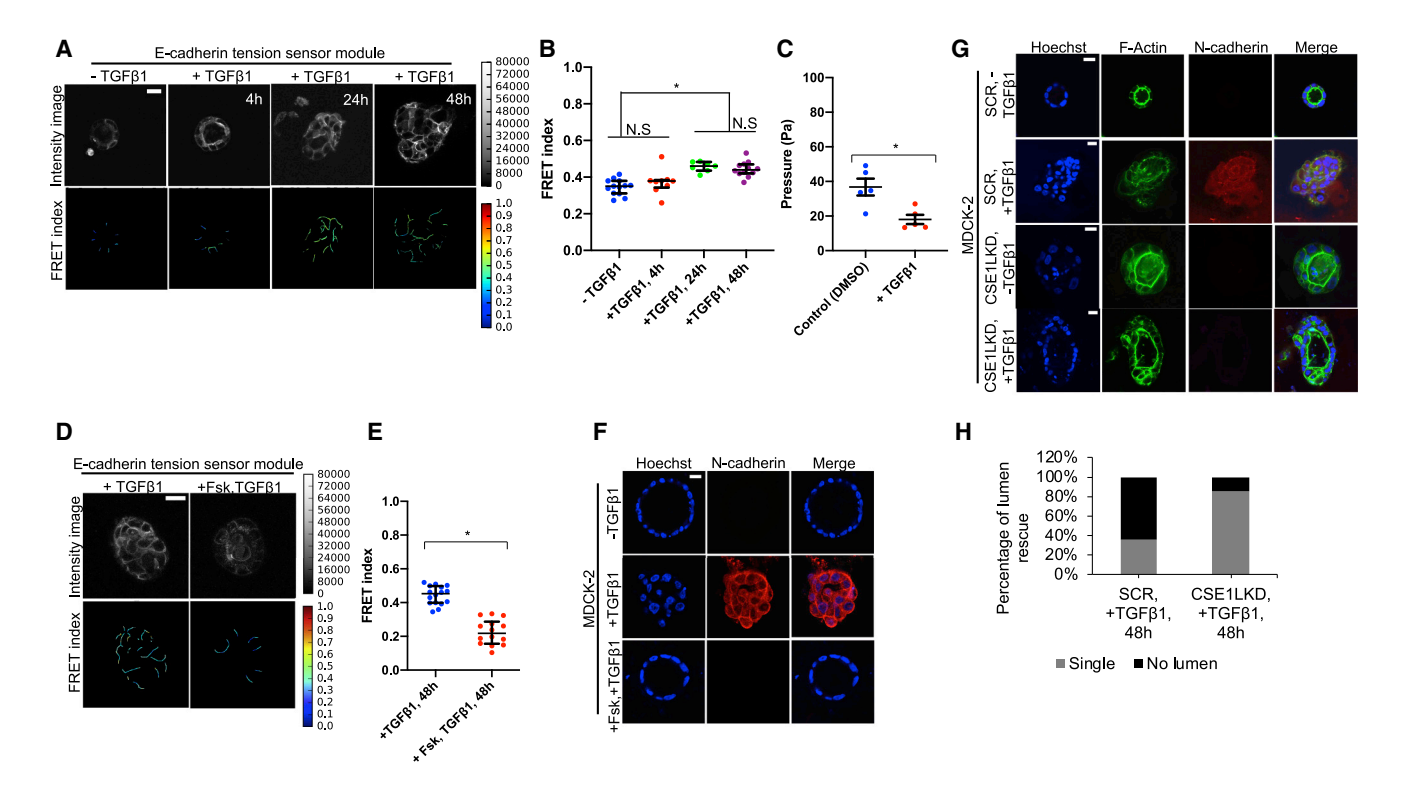


Figure 5. Force across E-cadherin Is Reduced during EMT Progression

(A) Time course of TGF-\(\beta\)1 treatment shows a gradual decrease in force across E-cadherin. Separate acini (expressing the E-cadherin tension sensor module) were imaged for each case (scale bar, 20 um).

(B) FRET index measurements as depicted in the scatter dot plot showed significant reduction in force across E-cadherin after 24 and 48 h of TGF-β1 treatment (2 ng-mL⁻¹) in the E-cadherin tension sensor module. The horizontal line (black) denotes the median of the FRET index estimates, and the black whiskers denote the largest observation within 1.5 x IQR (representative data shown are from one experiment chosen from a pool of at least three independent experiments that were performed on separate days; *p < 0.05; N.S, not significant, p > 0.05, one-way ANOVA and Mann-Whitney test).

- (C) Acini were cultured in Matrigel until they reached a luminal diameter of approximately 200 µm, and then pressure was measured following culture for 24 h in TGF-β1 (2 ng-mL⁻¹) and vehicle control (DMSO). At least 5 acini were measured for pressure in both cases (*p < 0.001, Student's t test).
- (D) Treatment of E-cadherin tension sensor module acini simultaneously with 10 µM Fsk (beginning 30 min prior to 48 h of 2 ng-mL⁻¹ TGF-β1 treatment) prevented the decrease in force across E-cadherin (as depicted by reduced FRET index) and preserved the single-lumen morphology (scale bar, 20 µm).
- (E) Mechanical tension across E-cadherin is significantly increased (decreased FRET index) with simultaneous treatment with Fsk, as shown in the scatter dot plot. The horizontal line (black) denotes the median of the FRET index estimates, and the black whiskers denote the largest observation within 1.5 x IQR (representative data shown are from one experiment chosen from a pool of three independent experiments that were performed on separate days; *p < 0.05, Mann-Whitney test).
- (F) Simultaneous treatment with 10 μM Fsk prevented TGF-β1 (2 ng-mL⁻¹) induced expression of N-cadherin (red) as well as acinar luminal filling (performed on the non-transfected parental MDCK-2 cells). Scale bar, 20 μm .
- (G) The CSE1LKD prototype of the non-transfected parental MDCK-2 cell-line displayed minimal N-cadherin (red) expression at the cell-cell junctions in the presence of TGF-β1 (2 ng-ml⁻¹) for 48 h, compared to its non-silenced scramble control (SCR) that was characterized by acinar luminal filling and increased N-cadherin expression (scale bars, 20 um).
- (H) Quantification of the CSE1LKD prototype for single-lumen morphology in the presence of TGF-β1 (2 ng-mL⁻¹) for 48 h. The majority of the CSE1LKD acini exhibited single lumens in the presence of TGF-β1 as opposed to its non-silenced scramble control. At least 15 acini were scored.

See also Figure S5 to further understand how increased CFTR activity blocks EMT progression in epithelial acini.

(present in both monolayers and acini). Epac1 activation blocked TGFβ1-induced N-cadherin expression in both 2D and 3D conditions, suggesting that its effects are independent of osmotic pressure (Figures S5E and S5F). However, activation of PKA with 6-Bnz-cAMP (an agonist that selectively activates cAMPdependent PKA but not Epac signaling pathways [34]) blocked EMT in 3D but not 2D conditions, indicating that its effect on EMT is likely due to increased osmotic pressure (Figures S5E and S5F). Knockdown of CSE1L also prevented TGFβ1-induced expression of N-cadherin and lumen filling in acini (Figures 5G and 5H).

DISCUSSION

It is well established that epithelial acini behave differently than 2D epithelial monolayers, which includes changes in morphology, apico-basal polarity, and responses to growth factors [1, 2]. In addition, innovative work by Valerie Weaver's group has shown that acini are responsive to changes in the extracellular environment [35]. However, it is not yet well understood how cells in acini experience and generate forces, particularly when grown in soft/compliant matrices like Matrigel. Traditionally, resistance from substrate stiffness is thought to be necessary for cells to generate large forces. Our data suggest that hydrostatic pressure can serve a similar resistance function, acting as a balance for intracellular myosin forces.

Our work in this study demonstrates that epithelial acini have significant lumen pressure and that this pressure (sensed as tensile forces by cells) affects the morphogenesis and homeostasis of acini. Our work in this paper adds to a growing body showing that pressure impacts cellular behavior. Within individual cells, changes in intracellular pressure have already been shown to be important for driving cell rounding during mitosis [36] and cell migration [37]. Likewise, forces from inter-blastocoelic hydrostatic pressure have shown to be important for fibronectin fibril assembly [38], formation and positioning of the blastocoel [39], and the control of blastocyst size [40]. Perhaps, most directly related to our studies of epithelial cells is a recent report showing the regulation of branching morphogenesis by transmural pressure in a developing lung [3]. Our study clearly demonstrates that mechanical forces (between and within cells) are affected by changes in ion secretion (Figure 2). Additionally, a recent report showed that basally formed hemicysts (also known as epithelial domes) also experience significant hydrostatic pressure [41]. The contribution of ionic gradients (osmotic pressure) to cellular forces should, therefore, be considered in any closed 3D cellular system in which fluid is

A number of studies have established that CFTR activity regulates the lumen size of epithelial acini [5, 6]. Based on the relationship between CFTR activity and lumen size, a previous hypothesis was that increases in apical delivery of ions by pumps and channels increase pressure within the lumen [8]. As indicated in Figure 3, by directly measuring pressure, we are able to directly demonstrate that CFTR chloride secretion contributes to the formation of lumen pressure, providing experimental validation of this prior hypothesis. Interestingly, further increases of CFTR did not result in increased lumen pressure, despite increasing E-cadherin force (Figure 2). Instead, increased CFTR activity resulted in a large increase in lumen size. According to the physical principle known as the law of Laplace, an increase in circumferential tension (E-cadherin force) can occur from either increased pressure or increased lumen volume. However, because the cells in the wall can also actively respond in ways to affect both pressure (e.g., ion secretion, changes in barrier function) and wall expansion (e.g., cell division, cytoskeletal changes, myosin contractility), the physical principles governing pressure, circumferential tension, and lumen expansion, and their correlations are likely more complex than predicted by the law of Laplace.

Given our observation of a plateau in pressure, it is tempting to speculate that acini may possess an internal pressure set point, which is mediated through an active feedback mechanism in which circumferential tension regulates cellular expansion (through changes in cellular elasticity, contractility, and cellular division), thereby establishing a homeostatic equilibrium. The mechanisms that could actively regulate acini expansion are not yet clear. Of note, recent work by Xavier Trepat's group has shown that epithelial cell expansion is not homogeneous and that some cells may possess super-elastic properties, allowing for some cells to rapidly expand into a super-stretched state [41]. It will be interesting to determine how cellular changes

can affect the relationship between pressure, tension, and expansion during more complex 3D morphological changes, such as tubulogenesis or branching morphogenesis.

Interestingly, despite mature acini being relatively homeostatic, our data also show variations in internal pressure (ranging from 21 to 49 Pa) (Figure 3A) and E-cadherin FRET measurements. We hypothesize that the pressure and circumferential tension of epithelial acini may be dynamic, being affected by a number of processes that occur even in mature acini (cell division, apoptosis, lumen size, paracellular leak, and changes in ion secretion).

Our work identifies the adherens junction as a potential sensor of tension arising from CFTR-driven ionic gradients. E-cadherin forces appear necessary for epithelial cells to respond to changes in osmotic pressure, including cellular proliferation (Figure 4). We also want to note that our 3D studies of CFTR-induced proliferation (Figure 4) complement a number of existing studies by James Nelson's group, in which it was shown that mechanical forces across E-cadherin are responsible for stretch-induced proliferation of epithelial 2D monolayers [32]. Given recent work by this group showing that increased tension on E-cadherin orients the direction of cell division [42], it is an attractive hypothesis that osmotic-pressure-induced E-cadherin forces could be a principal mechanism for maintaining the symmetric division of cells in acini.

Although our data support the hypothesis wherein circumferential stretch is sensed by the adherens junction, other mechanosensitive structures could ultimately be the primary mechanosensor. Our efforts to manipulate ionic gradients likely also affect forces across other structures in the cell-cell junction, such as desmosomes [43] and tight junctions [44], as well as other cytoskeletal connected structures, such as focal adhesions [19] and/or the nuclear LINC (linker of nucleoskeleton and cytoskeleton) complex [45].

Our finding of reduced force on E-cadherin, as well as lumen pressure, during the earliest stages of EMT (Figures 5A-5C) is surprising, given prior work suggesting that higher external forces (e.g., matrix stiffness) and intracellular forces (e.g., myosin contractility) promote EMT [35, 46, 47]. However, these prior results are not necessarily contradictory to our observations; rather, it is possible that EMT induces a transfer of force from cell-cell junctions to cell-matrix adhesions. Our findings are also supported by recent work showing that hepatocyte growth factor (HGF) stimulation (also known to induce EMT) decreases E-cadherin force [23]. In addition, it may be necessary to reduce force across E-cadherin to induce disassembly of adherens junctions, as E-cadherin has been shown to exhibit catch bond behavior [48]. Interestingly, loss of CFTR activity has also been shown to promote EMT [49]. Our work, along with other reports [50], indicates that cellular tension is an important factor in the propensity of cells to undergo EMT.

In conclusion, we show that epithelial acini experience significantly higher forces across E-cadherin, when grown in 3D, which arise from the effect of ionic gradients in the closed lumen. These forces are necessary for the formation and homeostasis of epithelial acini. Force biosensors such as TSmod are well suited for the study of mechanical forces in acinar structures and can be applied in future studies involving more complex 3D cellular systems.



STAR*METHODS

Detailed methods are provided in the online version of this paper and include the following:

- KEY RESOURCES TABLE
- LEAD CONTACT AND MATERIALS AVAILABILITY
- EXPERIMENTAL MODEL AND SUBJECT DETAILS
 - Stable cell lines
 - ShRNA knockdown
 - Cell culture and drug treatment
- METHOD DETAILS
 - Seeding in MatrigelTM for 3D live FRET imaging
 - FRET imaging and analysis
 - Immunostaining
 - Western Blotting
 - O Acini Pressure Measurements
 - O Acini size measurement
 - Acini compression
- QUANTIFICATION AND STATISTICAL ANALYSIS
- DATA AND CODE AVAILABILITY

SUPPLEMENTAL INFORMATION

Supplemental Information can be found online at https://doi.org/10.1016/j.cub.2019.12.025.

ACKNOWLEDGMENTS

We wish to thank Christopher Lemmon, Rebecca Heise, Gregory Walsh, Lewis Scott, Lauren Griggs, Kevin Denis, Shaston Newman, Jolene Cabe, Lynne Elmore, Venkat Maruthamuthu, Tanmay Lele, Alex Dunn, and Valerie Weaver for helpful discussions and Michel Bagnat, Alex Dunn, and Rob Tombes for providing reagents. We also especially acknowledge Andrei Ivanov for providing the initial suggestion of osmotic pressure affecting E-cadherin force and his guidance during the initial stages of the project. This project was supported by an Institutional Research grant IRG-73-001-37 from the American Cancer Society (to D.E.C.); a Burrows Welcome Fund grant 1017521 (to J.P.G.); a National Science Foundation CAREER award CMMI 1653299 (to D.E.C.); a National Science Foundation grant CMMI 1537256 (to J.P.G.); and grants R03AR068096 (to D.E.C.), R35GM119617 (to D.E.C.), R01HL133163 (to J.P.G.), and T32EB003392 (to T.J.A.) from NIH. Services and products in support of the research project were generated by the VCU Massey Cancer Center Biological Macromolecule Shared Resource supported, in part, with funding from NIH-NCI Cancer Center support grant P30 CA016059.

AUTHOR CONTRIBUTIONS

V.N. and L.E.S. designed and performed experiments and interpreted results. C.R.M., A.A.D., J.P.G., T.J.A., K.N.D., P.T.A., and A.M. designed experiments and interpreted results. D.E.C. and V.N. wrote the manuscript, with support from L.E.S., C.R.M., K.N.D., and J.P.G.

DECLARATION OF INTERESTS

The authors declare no competing interests.

Received: March 11, 2019 Revised: October 4, 2019 Accepted: December 9, 2019 Published: January 23, 2020

REFERENCES

- Zegers, M.M.P., O'Brien, L.E., Yu, W., Datta, A., and Mostov, K.E. (2003).
 Epithelial polarity and tubulogenesis in vitro. Trends Cell Biol. 13, 169–176.
- Underwood, J.M., Imbalzano, K.M., Weaver, V.M., Fischer, A.H., Imbalzano, A.N., and Nickerson, J.A. (2006). The ultrastructure of MCF-10A acini. J. Cell. Physiol. 208, 141–148.
- Nelson, C.M., Gleghorn, J.P., Pang, M.-F., Jaslove, J.M., Goodwin, K., Varner, V.D., Miller, E., Radisky, D.C., and Stone, H.A. (2017). Microfluidic chest cavities reveal that transmural pressure controls the rate of lung development. Development 144, 4328–4335.
- Desmond, M.E., and Jacobson, A.G. (1977). Embryonic brain enlargement requires cerebrospinal fluid pressure. Dev. Biol. 57, 188–198.
- Anderson, M.P., Gregory, R.J., Thompson, S., Souza, D.W., Paul, S., Mulligan, R.C., Smith, A.E., and Welsh, M.J. (1991). Demonstration that CFTR is a chloride channel by alteration of its anion selectivity. Science 253, 202–205.
- Navis, A., and Bagnat, M. (2015). Developing pressures: fluid forces driving morphogenesis. Curr. Opin. Genet. Dev. 32, 24–30.
- Alzamora, R., King, J.D., Jr., and Hallows, K.R. (2011). CFTR regulation by phosphorylation. Cystic Fibrosis (Humana Press), pp. 471–488.
- Datta, A., Bryant, D.M., and Mostov, K.E. (2011). Molecular regulation of lumen morphogenesis. Curr. Biol. 21, R126–R136.
- Ruiz-Herrero, T., Alessandri, K., Gurchenkov, B.V., Nassoy, P., and Mahadevan, L. (2017). Organ size control via hydraulically gated oscillations. Development 144, 4422–4427.
- Dasgupta, S., Gupta, K., Zhang, Y., Viasnoff, V., and Prost, J. (2018).
 Physics of lumen growth. Proc. Natl. Acad. Sci. USA 115, E4751–E4757.
- 11. De Maio, A., Vega, V.L., and Contreras, J.E. (2002). Gap junctions, homeostasis, and injury. J. Cell. Physiol. 191, 269–282.
- Green, K.J., Getsios, S., Troyanovsky, S., and Godsel, L.M. (2010). Intercellular junction assembly, dynamics, and homeostasis. Cold Spring Harb. Perspect. Biol. 2, a000125.
- Jia, L., Liu, F., Hansen, S.H., Ter Beest, M.B.A., and Zegers, M.M.P. (2011). Distinct roles of cadherin-6 and E-cadherin in tubulogenesis and lumen formation. Mol. Biol. Cell 22, 2031–2041.
- Marciano, D.K., Brakeman, P.R., Lee, C.-Z., Spivak, N., Eastburn, D.J., Bryant, D.M., Beaudoin, G.M., 3rd, Hofmann, I., Mostov, K.E., and Reichardt, L.F. (2011). p120 catenin is required for normal renal tubulogenesis and glomerulogenesis. Development 138, 2099–2109.
- Petrova, Y.I., Spano, M.M., and Gumbiner, B.M. (2012). Conformational epitopes at cadherin calcium-binding sites and p120-catenin phosphorylation regulate cell adhesion. Mol. Biol. Cell 23, 2092–2108.
- Pollack, A.L., Runyan, R.B., and Mostov, K.E. (1998). Morphogenetic mechanisms of epithelial tubulogenesis: MDCK cell polarity is transiently rearranged without loss of cell-cell contact during scatter factor/hepatocyte growth factor-induced tubulogenesis. Dev. Biol. 204, 64–79.
- Mohan, A., Schlue, K.T., Kniffin, A.F., Mayer, C.R., Duke, A.A., Narayanan, V., Arsenovic, P.T., Bathula, K., Danielsson, B.E., Dumbali, S.P., et al. (2018). Spatial proliferation of epithelial cells is regulated by E-cadherin force. Biophys. J. 115, 853–864.
- Borghi, N., Sorokina, M., Shcherbakova, O.G., Weis, W.I., Pruitt, B.L., Nelson, W.J., and Dunn, A.R. (2012). E-cadherin is under constitutive actomyosin-generated tension that is increased at cell-cell contacts upon externally applied stretch. Proc. Natl. Acad. Sci. USA 109, 12568–12573.
- Grashoff, C., Hoffman, B.D., Brenner, M.D., Zhou, R., Parsons, M., Yang, M.T., McLean, M.A., Sligar, S.G., Chen, C.S., Ha, T., and Schwartz, M.A. (2010). Measuring mechanical tension across vinculin reveals regulation of focal adhesion dynamics. Nature 466, 263–266.
- Xian, W., Schwertfeger, K.L., Vargo-Gogola, T., and Rosen, J.M. (2005).
 Pleiotropic effects of FGFR1 on cell proliferation, survival, and migration in a 3D mammary epithelial cell model. J. Cell Biol. 171, 663–673.

- Pearson, J.F., Hughes, S., Chambers, K., and Lang, S.H. (2009). Polarized fluid movement and not cell death, creates luminal spaces in adult prostate epithelium. Cell Death Differ. 16, 475–482.
- Soofi, S.S., Last, J.A., Liliensiek, S.J., Nealey, P.F., and Murphy, C.J. (2009). The elastic modulus of Matrigel as determined by atomic force microscopy. J. Struct. Biol. 167, 216–219.
- Gayrard, C., Bernaudin, C., Déjardin, T., Seiler, C., and Borghi, N. (2018).
 Src- and confinement-dependent FAK activation causes E-cadherin relaxation and β-catenin activity. J. Cell Biol. 217, 1063–1077.
- Conway, D.E., Breckenridge, M.T., Hinde, E., Gratton, E., Chen, C.S., and Schwartz, M.A. (2013). Fluid shear stress on endothelial cells modulates mechanical tension across VE-cadherin and PECAM-1. Curr. Biol. 23, 1024–1030.
- Haws, C.M., Nepomuceno, I.B., Krouse, M.E., Wakelee, H., Law, T., Xia, Y., Nguyen, H., and Wine, J.J. (1996). Delta F508-CFTR channels: kinetics, activation by forskolin, and potentiation by xanthines. Am. J. Physiol. 270, C1544-C1555.
- Ma, T., Thiagarajah, J.R., Yang, H., Sonawane, N.D., Folli, C., Galietta, L.J.V., and Verkman, A.S. (2002). Thiazolidinone CFTR inhibitor identified by high-throughput screening blocks cholera toxin-induced intestinal fluid secretion. J. Clin. Invest. 110, 1651–1658.
- Bagnat, M., Navis, A., Herbstreith, S., Brand-Arzamendi, K., Curado, S., Gabriel, S., Mostov, K., Huisken, J., and Stainier, D.Y.R. (2010). Cse1I is a negative regulator of CFTR-dependent fluid secretion. Curr. Biol. 20, 1840–1845.
- 28. Behrens, P., Brinkmann, U., and Wellmann, A. (2003). CSE1L/CAS: its role in proliferation and apoptosis. Apoptosis 8, 39–44.
- Jiang, M.-C., Liao, C.-F., and Tai, C.-C. (2002). CAS/CSE 1 stimulates E-cadhrin-dependent cell polarity in HT-29 human colon epithelial cells. Biochem. Biophys. Res. Commun. 294, 900–905.
- Li, H., Findlay, I.A., and Sheppard, D.N. (2004). The relationship between cell proliferation, CI- secretion, and renal cyst growth: a study using CFTR inhibitors. Kidney Int. 66, 1926–1938.
- Grantham, J.J., Uchic, M., Cragoe, E.J., Jr., Kornhaus, J., Grantham, J.A., Donoso, V., Mangoo-Karim, R., Evan, A., and McAteer, J. (1989). Chemical modification of cell proliferation and fluid secretion in renal cysts. Kidney Int. 35, 1379–1389.
- Benham-Pyle, B.W., Pruitt, B.L., and Nelson, W.J. (2015). Mechanical strain induces E-cadherin-dependent Yap1 and β-catenin activation to drive cell cycle entry. Science 348, 1024–1027.
- Insel, P.A., Murray, F., Yokoyama, U., Romano, S., Yun, H., Brown, L., Snead, A., Lu, D., and Aroonsakool, N. (2012). cAMP and Epac in the regulation of tissue fibrosis. Br. J. Pharmacol. 166, 447–456.
- 34. Poppe, H., Rybalkin, S.D., Rehmann, H., Hinds, T.R., Tang, X.-B., Christensen, A.E., Schwede, F., Genieser, H.-G., Bos, J.L., Doskeland, S.O., et al. (2008). Cyclic nucleotide analogs as probes of signaling pathways. Nat. Methods 5, 277–278.
- Paszek, M.J., Zahir, N., Johnson, K.R., Lakins, J.N., Rozenberg, G.I., Gefen, A., Reinhart-King, C.A., Margulies, S.S., Dembo, M., Boettiger, D., et al. (2005). Tensional homeostasis and the malignant phenotype. Cancer Cell 8, 241–254.
- Stewart, M.P., Helenius, J., Toyoda, Y., Ramanathan, S.P., Muller, D.J., and Hyman, A.A. (2011). Hydrostatic pressure and the actomyosin cortex drive mitotic cell rounding. Nature 469, 226–230.
- Petrie, R.J., Koo, H., and Yamada, K.M. (2014). Generation of compartmentalized pressure by a nuclear piston governs cell motility in a 3D matrix. Science 345, 1062–1065.

- Dzamba, B.J., Jakab, K.R., Marsden, M., Schwartz, M.A., and DeSimone, D.W. (2009). Cadherin adhesion, tissue tension, and noncanonical Wnt signaling regulate fibronectin matrix organization. Dev. Cell 16, 421–432.
- Dumortier, J.G., Le Verge-Serandour, M., Tortorelli, A.F., Mielke, A., de Plater, L., Turlier, H., and Maître, J.-L. (2019). Hydraulic fracturing and active coarsening position the lumen of the mouse blastocyst. Science 365, 465–468.
- Chan, C.J., Costanzo, M., Ruiz-Herrero, T., Mönke, G., Petrie, R.J., Bergert, M., Diz-Muñoz, A., Mahadevan, L., and Hiiragi, T. (2019). Hydraulic control of mammalian embryo size and cell fate. Nature 571, 112–116.
- Latorre, E., Kale, S., Casares, L., Gómez-González, M., Uroz, M., Valon, L., Nair, R.V., Garreta, E., Montserrat, N., Del Campo, A., et al. (2018). Active superelasticity in three-dimensional epithelia of controlled shape. Nature 563, 203–208.
- Hart, K.C., Tan, J., Siemers, K.A., Sim, J.Y., Pruitt, B.L., Nelson, W.J., and Gloerich, M. (2017). E-cadherin and LGN align epithelial cell divisions with tissue tension independently of cell shape. Proc. Natl. Acad. Sci. USA 114, E5845–E5853.
- 43. Baddam, S.R., Arsenovic, P.T., Narayanan, V., Duggan, N.R., Mayer, C.R., Newman, S.T., Abutaleb, D.A., Mohan, A., Kowalczyk, A.P., and Conway, D.E. (2018). The desmosomal cadherin desmoglein-2 experiences mechanical tension as demonstrated by a FRET-based tension biosensor expressed in living cells. Cells 7, 66.
- Spadaro, D., Le, S., Laroche, T., Mean, I., Jond, L., Yan, J., and Citi, S. (2017). Tension-dependent stretching activates ZO-1 to control the junctional localization of its interactors. Curr. Biol. 27, 3783–3795.e8.
- Arsenovic, P.T., Ramachandran, I., Bathula, K., Zhu, R., Narang, J.D., Noll, N.A., Lemmon, C.A., Gundersen, G.G., and Conway, D.E. (2016). Nesprin-2G, a component of the nuclear LINC complex, is subject to myosindependent tension. Biophys. J. 110, 34–43.
- Butcher, D.T., Alliston, T., and Weaver, V.M. (2009). A tense situation: forcing tumour progression. Nat. Rev. Cancer 9, 108–122.
- Levental, K.R., Yu, H., Kass, L., Lakins, J.N., Egeblad, M., Erler, J.T., Fong, S.F.T., Csiszar, K., Giaccia, A., Weninger, W., et al. (2009). Matrix crosslinking forces tumor progression by enhancing integrin signaling. Cell 139, 891–906.
- Manibog, K., Li, H., Rakshit, S., and Sivasankar, S. (2014). Resolving the molecular mechanism of cadherin catch bond formation. Nat. Commun. 5, 3941.
- 49. Zhang, J.T., Jiang, X.H., Xie, C., Cheng, H., Da Dong, J., Wang, Y., Fok, K.L., Zhang, X.H., Sun, T.T., Tsang, L.L., et al. (2013). Downregulation of CFTR promotes epithelial-to-mesenchymal transition and is associated with poor prognosis of breast cancer. Biochim. Biophys. Acta 1833, 2961–2969.
- Gomez, E.W., Chen, Q.K., Gjorevski, N., and Nelson, C.M. (2010). Tissue geometry patterns epithelial-mesenchymal transition via intercellular mechanotransduction. J. Cell. Biochem. 110, 44–51.
- Schneider, C.A., Rasband, W.S., and Eliceiri, K.W. (2012). NIH Image to ImageJ: 25 years of image analysis. Nat. Methods 9, 671–675.
- **52.** R Development Core Team (2018). R: a language and environment for statistical computing (R Foundation for Statistical Computing).
- **53.** Debnath, J., Muthuswamy, S.K., and Brugge, J.S. (2003). Morphogenesis and oncogenesis of MCF-10A mammary epithelial acini grown in three-dimensional basement membrane cultures. Methods *30*, 256–268.
- Jelínek, R., and Pexiedner, T. (1968). The pressure of encephalic fluid in chick embryos between the 2nd and 6th day of incubation. Physiol. Bohemoslov. 17, 297–305.



STAR***METHODS**

KEY RESOURCES TABLE

REAGENT or RESOURCE	SOURCE	IDENTIFIER
Antibodies		
Mouse monoclonal anti-N-Cadherin, clone 32	BD Biosciences	Cat# 610920; RRID: AB_2077527
Rabbit polyclonal anti-Twist1	Millipore	Cat# ABD29; RRID: AB_10807559
Rabbit monoclonal anti-E-Cadherin (24E10)	Cell Signaling Technology	Cat# 3195; RRID: AB_2291471
Mouse monoclonal anti-α-Smooth Muscle Actin, clone 1A4	Sigma-Aldrich	Cat# A5228; RRID: AB_262054
Mouse monoclonal anti-Vimentin (RV202)	Santa Cruz Biotechnologies	Cat# sc-32322; RRID: AB_628436
Mouse monoclonal anti-YAP (63.7)	Santa Cruz Biotechnologies	Cat# sc-101199; RRID: AB_1131430
Mouse monoclonal anti-YAP (M01), clone 2F12	Abnova	Cat#H00010413-M01; RRID: AB_535096
Rabbit polyclonal anti-Ki67	Thermo Fisher Scientific	Cat# PA5-19462; RRID: AB_10981523
Rabbit polyclonal anti-Ki67	Abcam	Cat# ab15580; RRID: AB_443209
Rabbit polyclonal anti-CSE1L	Bethyl Laboratories	Cat# A300-473A; RRID: AB_451008
Alexa Fluor 568 donkey anti-rabbit antibody	Thermo Fisher Scientific	Cat# A-10042; RRID: AB_2534017
Alexa Fluor 647 donkey anti-mouse antibody	Molecular Probes	Cat# A-31571; RRID: AB_162542
Alexa Fluor 647 chicken anti-rabbit antibody	Thermo Fisher Scientific	Cat# A-21443; RRID: AB_2535861
Alexa Fluor 488 goat anti-rabbit antibody	Molecular Probes	Cat# A-11008; RRID: AB_143165
Chemicals, Peptides, and Recombinant Proteins	-	
Matrigel Matrix Basement Membrane	Corning	Product#35623
Forskolin	Tocris	Cat#1099
CFTR _{inh} 172	Tocris	Cat#3430
Ouabain	Tocris	Cat#1076
B-Bromo-cAMP, sodium salt	Tocris	Cat#1140
6-Bnz-cAMP, sodium salt	Tocris	Cat#5255
B-pCPT-2-O-Me-cAMP-AM	Tocris	Cat#4853
Recombinant Human TGF-β1	R&D Systems	Cat#240-B-002
Experimental Models: Cell Lines	-	
MDCK-2	Gifted by Rob Tombes (VCU Biology)	N/A
Recombinant DNA		
Full length canine E-cadherin TSmod	Gifted by Alex Dunn [18]	N/A
Canine E-cadherin Ecad∆cyto	Gifted by Alex Dunn [18]	N/A
Full length canine E-cadherin TSmod, dark mTFP1 Y72L in mTFP1)	Generated by site directed mutagenesis	N/A
Full length canine E-cadherin TSmod, dark mEYFP Y66L in mEYFP)	Generated by site directed mutagenesis	N/A
entivirus shRNA canine CSE1L	Gifted by Michel Bagnat [27]	N/A
non-silencing scramble shRNA pLKO.1	Gifted by Michel Bagnat [27]	Addgene#1864
Software and Algorithms	-	
mageJ	[51]	https://imagej.nih.gov/ij/
R Software	[52]	https://www.R-project.org/

LEAD CONTACT AND MATERIALS AVAILABILITY

Further information and requests for resources and reagents (including stable cell lines and other plasmids) should be directed to and will be fulfilled by the Lead Contact, Daniel E. Conway (dconway@vcu.edu). All unique/stable reagents generated in this study are available from the Lead Contact with a completed Materials Transfer Agreement.

EXPERIMENTAL MODEL AND SUBJECT DETAILS

Stable cell lines

To generate stable cell lines expressing canine full-length E-cad TSmod, and EcadΔcyto, cells were transfected with lipofectamine 2000 and selected using 500 ug/ml G418 (ThermoFisher). Full-length canine E-cad TSmod and EcadΔcyto, consisting of a modified TSmod (eYFP A206K instead of venus A206K) were gifted by Alex Dunn [18]. Dark mTFP1 and dark mEYFP versions of E-cad TSmod for intermolecular FRET controls were generated by site directed mutagenesis to change a single tyrosine (equivalent to Y66 in eGFP) to leucine [24].

ShRNA knockdown

CSE1L was knocked down using lentivirus shRNA canine CSE1L (pLKO.1 vector, sequence CCGG CCCTGCTGCTGTTGTAAAT CTCGAG ATTTACAA CAGCAGCAGGGTTTTTG, gift of Michel Bagnat) [27]. The non-silencing scramble shRNA pLKO.1 (addgene #1864, gift of Michel Bagnat) was used as a control. Cells were infected and then selected with 1.0 ug/ul puromycin. Knockdown was verified by western blotting, using rabbit CSE1L antibody (A300-473A, Bethyl Laboratories). Because CSE1L knockdown was not found to be stable, cells were used within 2-4 passages of infection.

Cell culture and drug treatment

Madin-Darby canine kidney cells (MDCK-2) were a gift from Rob Tombes (VCU Biology) and were maintained in high glucose DMEM (ThermoFisher) to which was added 10% fetal bovine serum (ThermoFisher) and 1% penicillin/streptomycin (ThermoFisher) under standard cell culture conditions. Madin-Darby canine kidney cells (MDCK-2) were grown in MatrigelTM for 7-10 days to form acini using the protocol of Debnath et al. [53]. Phenol-free reduced growth factor reduced MatrigelTM (Corning) was used for all 3D acini experiments. For experiments involving immunofluorescence staining, 8-well chamber slides were used (Lab-Tek, Rochester, NY) and for live-cell imaging experiments p-35 10 mm glass bottom dishes (#1.5 glass, Cell Vis, Mountain View, California). The pipettes and centrifuge tubes used for MatrigelTM and preparation of the seeding media were kept at 4°C. The matrigel bed was created from 45 μL of MatrigelTM, maintained at 4°C, followed by incubation at 37°C for 30 minutes to allow cross-linking of the gelatinous protein mixture [53]. The cells were sub-cultured and re-suspended in media and MatrigelTM and added to the chamber slides or glass bottom dishes. Cells were then incubated at 37°C for a period of 7-10 days, with media replacement every 3 days. Because CSE1L knockdown cells developed larger lumens in a shorter time span, these acini were imaged at an earlier time point (5 days), as indicated. For perturbation of CFTR activity, Forskolin (Tocris Bioscience, UK), the chloride channel inhibitor CFTR_{inh}-172 (Tocris Bioscience, UK), the chlor ence, UK), Epac1 activator 8-pCPT-2-O-Me-cAMP-AM (Tocris Bioscience, UK), and protein kinase A activators; 8-Bromo-cAMP, sodium salt and 6-Bnz-cAMP, sodium salt (Tocris Bioscience, UK) were each used at a working concentration of 10 μM in all experiments. To inhibit the basal Na*/K*-ATPase pump, Ouabain (Tocris Bioscience, UK) was used at a working concentration of 0.1 μM in all experiments. For experiments involving EMT induction, recombinant human TGF-β1 (R&D systems) was used at a concentration of 2 ng/ml in all experiments.

METHOD DETAILS

Seeding in MatrigelTM for 3D live FRET imaging

For live-cell imaging experiments, p-35 10 mm glass bottom dishes (#1.5 glass, Cell Vis, Mountain View, California) were used. In order to compare FRET-based force measurements in epithelial acini, 50 µL of MatrigelTM maintained at 4°C was used to create the matrigel bed, in such a way that the bed is thicker at the center and thinner along the rim of the p-35 10mm glass cut-out dishes. By tapering the bed toward the rim starting from the center in a circular pattern, a gradient in depth is created such that acini are formed in the areas that are deep enough for the cells to burrow in as a result of matrigel overlay. At the same time, the thinner areas of the bed form monolayers, thereby preventing acini formation, and were used for 3D versus 2D comparison studies. The matrigel bed was allowed to solidify as a result of cross-linking of the gelatinous protein mixture by incubation at 37°C for 30 minutes. The pipettes and centrifuge tubes used for MatrigelTM, and preparation of the seeding media were precooled at 4°C. The cells were sub-cultured and re-suspended in media and MatrigelTM, and about 300 ul of the seeding media containing the cells was added onto the 10mm cut-out area of the glass bottom dishes. DMEM media replenished with FBS and pen-strep was added 1-2 hours later and the dishes were incubated at 37°C for a period of 7-10 days, with media replacement every 3 days.

FRET imaging and analysis

Living cells in glass bottom dishes expressing the force sensors were imaged using a plan-apochromat 40x water immersion NA 1.1 objective lens on an inverted Zeiss LSM 710 laser scanning microscope (Oberkochen, Germany). All the images were acquired at 458 nm excitation wavelength from an argon laser source. Using the online-unmixing mode, both mTFP1 (donor) and mEYFP (acceptor) channels were collected via spectral unmixing as previously described [45].

Intensity images were further processed and analyzed using a custom Python code, which involved background subtraction and removal of saturated pixels, as previously described [45]. For each dataset, the data was acquired for at least 7-8 epithelial acini. Images were masked manually on ImageJ (Fiji). Because it is difficult to discern from the confocal image section if the E-cadherin is truly basal (or out of plane lateral), due to the acinus orientation in matrigel, all of the E-cadherin-positive cell membranes were



included in masked images. For some datasets, a more stringent masking approach (in which only obvious lateral junctions were masked) was employed compared to the more lenient masking (in which all E-cadherin-positive cell membranes were included). While it was observed that the strict masking approach was more precise, data presented in this manuscript are from images that were masked so as to include all possible E-cadherin-positive cell membrane.

The FRET index images were obtained by taking the ratio of the acceptor fluorophore channel (mEYFP) to the donor fluorophore channel (mTFP1), which was then multiplied with the binary image masks that outlined the cell-cell junctions in order to inspect FRET pixels of interest. When comparing multiple groups, all pixels of interest were aggregated following which, an upper and lower bound for the intensity was chosen in order to exclude dim pixels. Low intensity/dim pixels can bias the FRET index due to noise and autofluorescence, and bright pixels, on the other hand, can bias the FRET index due to detector saturation, as previously described by Arsenovic et al. [45]. The upper and lower bounds on the intensity were chosen based on the slope of the FRET index versus intensity behavior such that the plateau region of the plot is isolated and the same intensity bounds are applied to all groups in an experiment to prevent the choice of bounds from affecting the relative differences between groups.

Immunostaining

Immunofluorescence experiments were performed using the 8-well chamber slides. Antibodies used were: mouse monoclonal anti-N-Cadherin (clone 32, BD Biosciences, working dilution 1:200), rabbit polyclonal anti-Twist1 (ABD29, EMD Millipore, working dilution 1:50), rabbit monoclonal anti-E-Cadherin (24E10, Cell Signaling Technology, working dilution 1:200), rabbit polyclonal anti-CSE1L (A300-473A, Bethyl Laboratories, working dilution 1:1000), mouse monoclonal anti-α-Smooth Muscle Actin (A5228, Sigma-Aldrich, working dilution 1:200), mouse monoclonal anti-Vimentin (sc-32322, Santa Cruz Biotechnologies, working dilution 1:200), mouse monoclonal anti-YAP (sc-101199, Santa Cruz Biotechnologies, working dilution 1:100; and M01, clone 2F12, Abnova, working dilution 1:100), and rabbit polyclonal anti-Ki67 (PA5-19462, Thermo Fisher Scientific; and ab15580, Abcam; working dilution 1:500). Cells were fixed with 2% para-formaldehyde in Ca2+PBS and incubated at 37°C overnight. The samples were then rinsed thrice with PBSglycine (0.1M) to quench the aldehyde groups and permeabilized with 0.5% Triton X-100 (Sigma) for 30 minutes, followed by three additional 0.1M PBS-glycine rinses and blocking with 5% BSA (Sigma), all at room temperature. Primary antibodies were added and incubated at 4°C overnight and allowed to return to room temperature prior to the next series of steps that were performed in the dark at room temperature. Following three PBS rinses, the relevant secondary antibodies; Alexa Fluor 568 donkey anti-rabbit antibody, Alexa Fluor 647 donkey anti-mouse antibody (Thermo Fisher Scientific, working dilution 1:250), and Alexa Fluor 647 chicken anti-rabbit antibody, Alexa Fluor 488 goat anti-rabbit antibody (Molecular Probes, working dilution 1:250) were added and incubated at room temperature for one hour. In the indicated experiments, acini were co-stained with Acti-stain 488, phalloidin (Cytoskeleton, Inc.) and Hoechst 33342 (Thermo Fisher Scientific). Slides were mounted and imaged with a Zeiss LSM 710 confocal laser-scanning microscope.

Western Blotting

For the immunoblot, cells were plated on six wells and allowed to grow to confluency following which, the protein was extracted through cell lysis and quantified. Standard polyacrylamide gel electrophoresis and western blot procedures were employed using the BioRad Trans-Blot 20 Mini-Protean Tetra System, 4%–20% bis-acrylamide crosslinked gels, and polyvinylidene fluoride (PVDF) microporous membranes. Analysis of protein expression was conducted using either chemiluminescent images of PVDF membranes captured on the BioRad ChemiDoc Touch Gel Imaging System and associated Image Lab software.

Acini Pressure Measurements

Luminal pressure of MDCK acini was measured using a micropipette connected to a pressure transducer, as adapted from Jelinek and Pexiedner [54]. Briefly, borosilicate glass micropipettes were pulled to an internal diameter of 40-45 μ m with a 30° beveled tip and connected via polyethylene tubing to a differential pressure transducer (Honeywell; CPCL04DFC). A signal conditioner (Omega; DMD4059-DC) was used to amplify the transducer signal, and a data acquisition module (National Instruments; USB-6009) and custom LabVIEW program were used to record voltage over time. The transducer was calibrated using a water manometer and all data were processed in MATLAB.

MDCK-2 acini were cultured on MatrigelTM in PDMS wells adhered to glass coverslips until a diameter of approximately 200 μ m was achieved. Upon growing to the appropriate size, acini were treated with DMSO (control), forskolin (10 μ M), or CFTR_{inh}-172 (10 μ M), PKA (10 μ M), Ouabain (0.1 μ M) and TGF- β 1 (2 ng/ml) for 24 hours. Following culture, the micropipette tip was inserted into each spheroid after a five-minute voltage baseline was collected. The luminal pressure was recorded for at least five minutes before the micropipette was removed and pressure was recorded as the average pressure value over the time period. Pressures reported are relative pressures; the internal lumen pressure being relative to the pressure at the same height in the media outside of the acinus.

Acini size measurement

MDCK-2 acini were cultured in MatrigelTM and analyzed for luminal size changes upon forskolin treatment over a period of 24 hours compared to the untreated control. 5×5 grids were drawn out on the base of the 8-well chamber slides prior to seeding in order to aid in locating the same acinus over a 24-hour time frame. The major and minor axes were recorded using ImageJ and the corresponding elliptical area measurements for the central cross-section of an acinus was calculated. The percentage change in area (before and

after treatment) compared to the untreated control, was recorded and graphed in Microsoft excel. Since the same acinus was imaged over a period of 24 hours, a paired Student's t test statistical analysis was performed using the R software.

Acini compression

MDCK-2 cells expressing the wild-type E-cadherin sensor was allowed to form into acini over a period of 7 days in glass bottom p-35 dishes (as described in Seeding in MatrigelTM for 3D live FRET imaging). Spheroids closer to the 10mm cut-out wall were located using the Zeiss LSM 710 confocal laser-scanning microscope, with an image captured of the acinus prior to compression. The located acinus was compressed using a calibrated 20 g weight by applying it onto the matrigel bed, perpendicular to the xy-plane (Figure S3C). Acini compression was accomplished by moving the weight along the x- direction, against the 10mm cut-out wall. The linear force used to move the weight was applied by hand. A second image was captured of the same acinus while compressed. In order to detect the recoil, the weight was moved away, and a third image of the unloaded acinus was acquired. Each image was processed using Fiji (ImageJ), and area outlines as well as circularity measurements were obtained as a result, which included the major and minor axes measurements. The circularity measurements recorded for the two experiments involving the untreated control (- Fsk, CFTR(inh)172), CFTR-inhibited (+ CFTR(inh)172, 24h) and the forskolin-treated (+ Fsk, 24h) acini were plotted on MS Excel (Figures S3D, S3E and S3F).

To measure strain during compression and with release of compression, the (x,y) coordinates of 24 points were captured around the circumference of the acini with points 1, 7, 13, 19 at the four major poles and 5 points equidistant in between, using Fiji (xyclick macro). The mean edge strain was determined using MATLAB based on coordinate geometry, and the (x,y) points were aligned based on acini centroid and by eye to minimize overall difference between conditions (compression and release). Root mean squared displacements between conditions were then determined and averaged for acini (Figures S3G and S3H).

QUANTIFICATION AND STATISTICAL ANALYSIS

Statistical significance was measured using unpaired, two-tailed Student's t test, two-tailed Mann-Whitney test and the Analysis of Variance (ANOVA) test. The One-way ANOVA test was followed by a further comparison of the groups using the Tukey (HSD) test so as to obtain significant differences between multiple groups, if any. In the case of observations that are paired and imaged under varying conditions, a paired t test was conducted to obtain statistical significance. All statistical tests were conducted at a 5% significance level (p < 0.05). The R statistical software was used for statistical analyses.

DATA AND CODE AVAILABILITY

All data and code supporting the findings of this study are available from the corresponding author upon request.